VNU Journal of Science: Mathematics – Physics, Vol. 31, No. 4 (2015) 56-65

Zeta Potential Measurement Using Streaming Potential in Porous Media

Luong Duy Thanh[1,*], Rudolf Sprik[2]

[1]*Water Resources University, 175 Tay Son, Dong Da, Hanoi, Vietnam*
[2]*Van der Waals-Zeeman Institute, University of Amsterdam, The Netherlands*

Received 26 October 2015
Revised 17 November 2015; Accepted 23 December 2015

Abstract: Electrokinetic phenomena are induced by the relative motion between a fluid and a solid surface and are directly related to the existence of an electric double layer between the fluid and the solid grain surface. Electrokinetics in porous media plays an important role in geophysical applications and environmental applications. The zeta potential is one of the key parameters in electrokinetics. The zeta potential of liquid-rock systems depends on many parameters such as mineral composition of rocks, fluid properties etc. Therefore, the zeta potential is different for various rocks and liquids. In order to measure the zeta potential for fluid saturated porous rocks, streaming potential measurements have been carried out for 8 consolidated samples including natural and artificial rocks saturated with 7 different NaCl solutions. The measured zeta potential is then compared to previously published data for silica-based rocks. The comparison shows that the zeta potential is in good agreement with the experimental data reported in the literature. The results also indicate that the zeta potential depends not only on the electrolyte concentration but also on types of rock.

Keywords: Streaming potential, zeta potential, electroosmosis, porous media, rocks.

1. Introduction

The electrokinetic phenomena are induced by the relative motion between the fluid and the solid surface. In a porous medium such as rocks or soils, the electric current density, linked to the ions within the fluid, is coupled to the fluid flow and that coupling is called electrokinetics e.g. [1]. Electrokinetics consists of several different effects such as streaming potential, seismoelectrics, electroosmosis, electrophoresis etc. Electrokinetics plays an important role in geophysical applications, environmental applications, medical applications and others. For example, the streaming potential is used to map subsurface flow and detect subsurface flow patterns in oil reservoirs [2]. Streaming potential is also used to monitor subsurface flow in geothermal areas and volcanoes [3, 4,

*Corresponding author. Tel.: 84- 936946975
Email: luongduythanh2003@yahoo.com

5]. Monitoring of streaming potential anomalies has been proposed as a means of predicting earthquakes [6, 7] and detecting of seepage through water retention structures such as dams, dikes, reservoir floors, and canals [8]. Seismoelectric effects can be used in order to investigate oil and gas reservoirs [9], hydraulic reservoirs [10- 12].

Electroosmosis that arises due to the motion of liquid induced by an applied voltage across a porous material or a micro channel is one of the promising technologies for cleaning up low permeable soil in environmental applications. In this process, contaminants are separated by applying an electric field between two electrodes inserted in the contaminated mass. Therefore, it has been used for the removal of organic contaminants, petroleum hydrocarbons, heavy metals and polar organic contaminants in soils, sludge and sediments [13-15]. Additionally, electroosmosis has been used to produce microfluidic devices such as electroosmotic pumps (EOPs) with several outstanding features: EOPs are capable of generating constant and pulse-free flows, the flow magnitude and direction of EOPs are easy to control, EOPs have no moving parts. EOPs have been used in microelectronic equipment cooling, drug delivery [16].

The zeta potential of a solid-liquid interface of porous media is one of the most important parameters in electrokinetics. In general, zeta potential is measured indirectly using one of the techniques: streaming current or streaming potential, electroosmotic mobility, electrophoretic mobility measurements etc. [17]. Electrophoretic mobility measurement is common in studies of colloidal suspensions. The electroosmotic mobility is common in studies of nanofluidics and microfluidics. In this work, streaming potential measurements are used to determine the zeta potential for 8 consolidated samples including natural and artificial rocks saturated with 7 different NaCl solutions. The experimental results are then compared to previously published data for silica-based rocks. The comparison shows that the zeta potential is in good agreement with the experimental data reported in the literature. The results also indicate that the zeta potential depends not only on the electrolyte concentration but also on types of rock.

This paper includes five sections. Section 2 describes the theoretical background of streaming potential. Section 3 presents the experimental measurement. Section 4 contains the experimental results and discussion. Conclusions are provided in the final section.

2. Theoretical background of streaming potential

A porous medium is formed by mineral solid grains such as silicates, oxides, carbonates etc. When a solid grain surface is in contact with a liquid, it acquires a surface electric charge [20]. The surface charge repels ions in the electrolyte whose charges have the same sign as the surface charge (called the “coions”) and attracts ions whose charges have the opposite sign (called the ”counterions” and normally cations) in the vicinity of the electrolyte silica interface. This leads to the charge distribution known as the electric double layer (EDL) as shown in Fig. 1. The EDL is made up of the Stern layer, where cations are adsorbed on the surface and are immobile due to the strong electrostatic attraction, and the diffuse layer, where the ions are mobile. The distribution of ions and the electric potential within the diffuse layer is governed by the Poisson Boltzman (PB) equation which accounts for the

balance between electrostatic and thermal diffusion forces [20]. The solution to the linear PB equation in one dimension perpendicular to a broad planar interface is well-known and produces an electric potential profile that decays approximately exponentially with distance as shown in Fig. 1. In the bulk liquid, the number of cations and anions is equal so that it is electrically neutral. The closest plane to the solid surface in the diffuse layer at which flow occurs is termed the shear plane or the slipping plane, and the electrical potential at this plane is called the zeta potential (ζ). The zeta potential plays an important role in determining the degree of coupling between the electric flow and the fluid flow in porous media. Most reservoir rocks have a negative surface charge and a negative zeta potential when in contact with ground water [21, 22]. The characteristic length over which the EDL exponentially decays is known as the Debye length and is on the order of a few nanometers for typical grain electrolyte combinations [21].

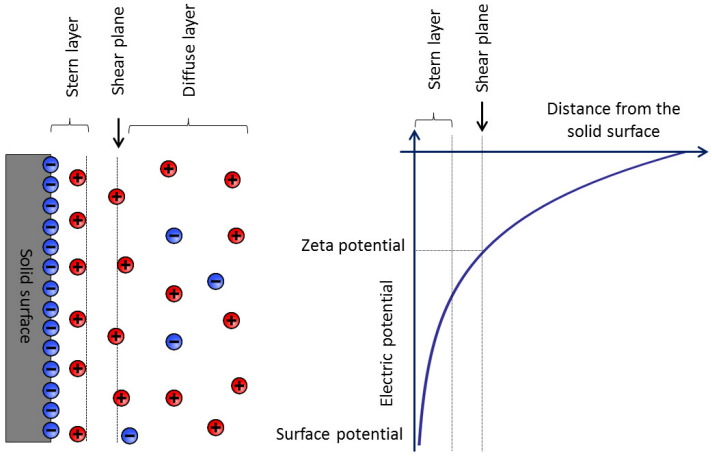

Figure 1. Stern model [18, 19] for the charge and electric potential distribution in the electric double layer at a solid-liquid interface. In this figure, the solid surface is negatively charged and the mobile counter-ions in the diffuse layer are positively charged (in most rock-water systems).

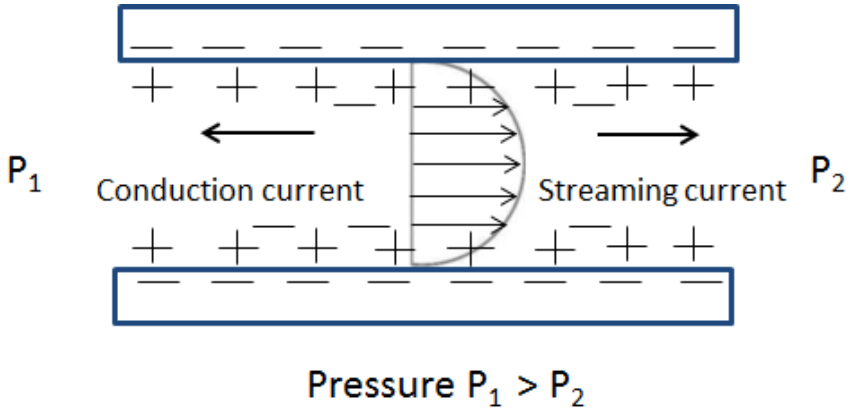

Figure 2. Development of streaming potential when an electrolyte is pumped through a capillary (a porous medium is made of an array of parallel capillaries).

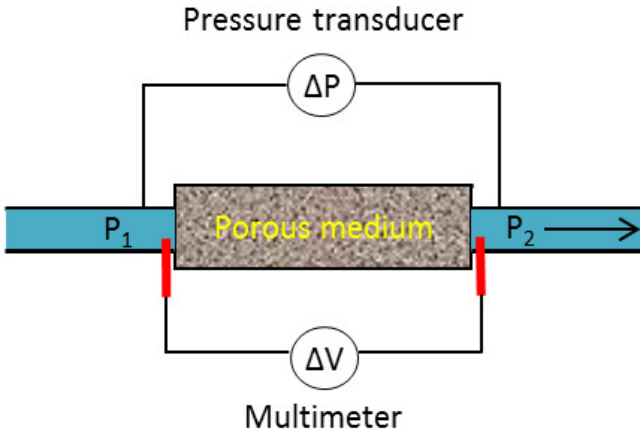

Figure 3. Schematic illustration of streaming potential measurement when an electrolyte is pumped through a porous medium. $\Delta V=V_{P1}-V_{P2}$ is the streaming potential and $\Delta P=P_{P1}-P_{P2}$ is the fluid pressure difference.

The streaming current is created by the relative motion of the diffuse layer with respect to the solid surface induced by a fluid pressure drop over the channel (a porous medium can be approximated as an array of parallel channels) and is directly related to the existence of an electric double layer (EDL) between the fluid and the solid surface as shown in Fig. 1. This streaming current is balanced by a conduction current, leading to the streaming potential (see Fig. 2). In a fluid saturated porous medium, the electric current density and the fluid flux are coupled, so fluids moving through porous media generate a streaming potential [24] (see Fig. 3). The streaming potential increases linearly with the fluid pressure difference that drives the fluid flow, provided that the flow remains laminar [25]. The steady state streaming potential coefficient (SPC) is defined when the total current density is zero as [1, 4]

$$C_S = \frac{\Delta V}{\Delta P} = \frac{\varepsilon_r \varepsilon_o \zeta}{\eta \sigma_{eff}}, \qquad (1)$$

where ΔV is the streaming potential, ΔP is the fluid pressure difference, ε_r is the relative permittivity of the fluid, ε_o is the dielectric permittivity in vacuum, η is the dynamic viscosity of the fluid, σ_{eff} is the effective conductivity, and ζ is the zeta potential. The effective conductivity includes the fluid conductivity and the surface conductivity. To characterize the relative contribution of the surface conductivity, the dimensionless quantity called the Dukhin number has been introduced [26]. The zeta potential is a function of many parameters including mineral composition of porous media, ionic species that are present in the fluid, the pH of fluid, fluid composition, fluid electrical conductivity and temperature etc. [21, 27]. The SPC can also be written as [28]

$$C_S = \frac{\varepsilon_r \varepsilon_o \zeta}{\eta F \sigma_r}, \qquad (2)$$

where σ_r is the electrical conductivity of the sample saturated by a fluid with a conductivity of σ_f and F is the formation factor. The electrical conductivity of the sample can possibly include surface

conductivity. If the fluid conductivity is much higher than the surface conductivity, the effective conductivity is approximately equal to the fluid conductivity, $\sigma_{eff} = F\sigma_r = \sigma_f$ and the SPC becomes the well-known Helmholtz-Smoluchowski equation:

$$C_S = \frac{\varepsilon_r \varepsilon_o \zeta}{\eta \sigma_f}. \quad (3)$$

3. Experiment

3.1. Materials

Streaming potential measurements have been performed on 8 consolidated samples that are all silica-based rocks. The natural samples numbered from 1 to 3 were obtained from Shell Oil Company in the Netherlands. Artificial samples numbered from 4 to 5 were obtained from HP Technical Ceramics Company in England. The natural samples numbered from 6 to 7 were obtained from Berea Sandstone Petroleum Cores Company in the US. The last one numbered 8 was obtained from Delft University in the Netherlands. The mineral composition and micro structure parameters (porosity, solid density, permeability and formation factor) have been reported in [32] and re-shown in table 1. NaCl solutions are used with 7 different concentrations (4.0×10^{-4} M, 1.0×10^{-3} M, 2.5×10^{-3} M, 5.0×10^{-3} M, 1.0×10^{-2} M, 2.0×10^{-2} M and 5.0×10^{-2} M). All measurements are carried out at room temperature (22 ± 1^{o}C).

Table 1. Sample ID, mineral compositions and microstructure parameters of the samples. Symbols k_o (in mD), Φ (in %) , F (no units), α_∞ (no units), ρ_s (in kg/m^3) stand for permeability, porosity, formation factor, tortuosity and solid density of porous media, respectively. For lithology, BER and BereaUS stand for Berea sandstone, BEN stands for Bentheim Sandstone, DP stands for artificial ceramic core.

	Sample ID	Mineral compositions	k_o	ϕ	F	α_∞	ρ_s
1	BER5	Silica (74.0-98.0%), Alumina and clays (see [29, 30])	51	21.1	14.5	3.1	2726
2	BER502	-	182	22.5	13.5	3.0	2723
3	BEN6	Mostly Silica (see [31])	1382	22.3	12.0	2.7	2638
4	DP50	Alumina and fused silica (see: www.tech-ceramics.co.uk)	2960	48.5	4.2	2.0	3546
5	DP46i	-	4591	48.0	4.7	2.3	3559
6	BereaUS1	Silica, Alumina, Ferric Oxide, Ferrous Oxide (www.bereasandstonecores.com)	120	14.5	19.0	2.8	2602
7	BereaUS5	-	310	20.1	14.5	2.9	2514
8	BEN7	Mostly Silica (see [31])	1438	22.2	12.6	2.8	2647

3.2. Experimental setup

The experimental setup for the measurement of the streaming potential is shown in Fig. 4 (for more details, see [33]). The core holder contains a cylindrical sample of 55 mm in length and 25 mm in diameter (Fig. 5). Each sample is surrounded by a 4 mm thick silicone sleeve inside a conical

stainless steel cell and inserted into a stainless steel holder to prevent flow a long the interface of the sample. The solution is circulated through the samples until the electrical conductivity and pH of the solution reach a stable value measured by a multimeter (Consort C861). The pH values of equilibrium solutions are in the range 6.0 to 7.5. Electrical potential differences across the samples are measured by a high input impedance multimeter (Keithley Model 2700) connected to a computer and controlled by a Labview program (National Instruments). The input resistance of the multimeter is larger than 10GΩ. The resistance of the saturated samples is smaller than 200kΩ, which is low compared to input resistance of the multimeter, therefore allowing accurate measurements of electric potentials. Pressure differences across a sample are measured by a high-precision differential pressure transducer (Endress and Hauser Deltabar S PMD75).

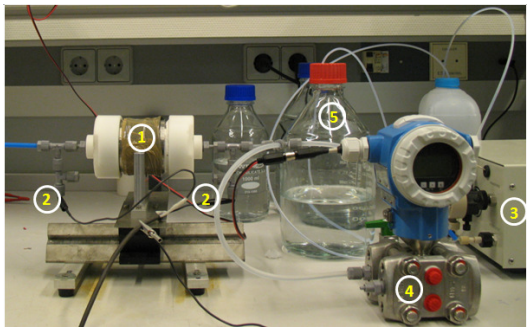

Figure 4. Experimental setup for streaming potential measurements. 1, Core holder; 2, Ag/AgCl electrodes; 3, Pump; 4, Pressure transducer; 5, NaCl solution container.

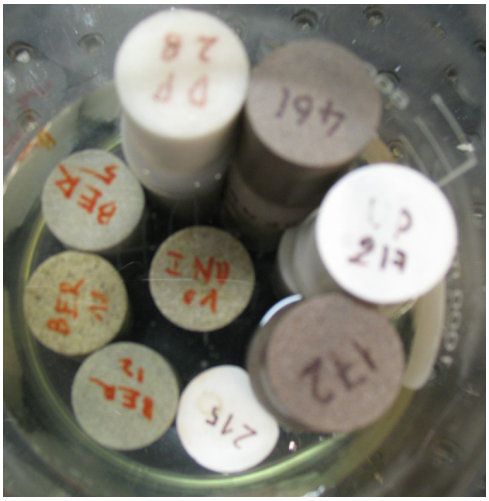

Figure 5. Consolidated samples.

3.3. Zeta potential measurement

The way used to collect the SPC is similar to that described in [32, 33] where Ag/AgCl electrodes are used to avoid polarization. In our measurements, Ag/AgCl wire electrodes are bought from a

manufacturer of A-M systems. Fig. 6 shows an example of the streaming potential as a function of time when the pressure difference is switched from 0.72 bar to 0.94 bar at electrolyte concentration of 5.0×10^{-2}M (see the inset). From that, the streaming potential as a function of pressure difference and therefore, the SPC as the slope of the straight line are obtained as shown in Fig. 6. The fluctuation of electrical potential difference at a given pressure difference (see the inset of Fig. 6) could be partly due to periodic pulses of the pump when the piston switches its direction after half a period. The frequency of the pump depends on the flow rate that we need to apply to generate fluid pressure differences (the higher pressure difference, the larger frequency). Three measurements are performed for all samples with each solution to find the average value of the SPC.

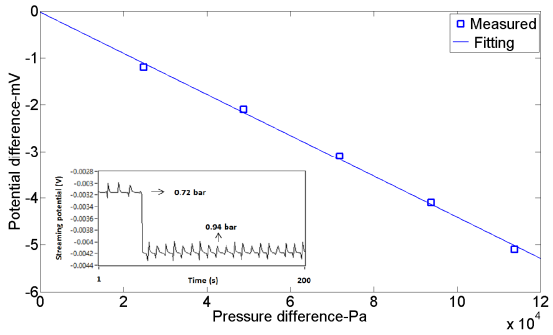

Figure 6. Streaming potential as a function of pressure difference for BereaUS5 at a concentration of 5.0×10^{-2} M. The inset shows an example of streaming potentials as a function of time at when pressure difference is switched from 0.72 bar to 0.94 bar.4. Results and discussion

Table 2. The streaming potential coefficient (in mV/bar) for different electrolyte concentrations.

	Sample ID	0.4 mM	1 mM	2.5 mM	5 mM	10 mM	20 mM	50 mM
1	BER5	-82.0	-56.0	-35.0	-21.0	-12.5	-7.0	-3.2
2	BER502	-130.0	-85.0	-46.0	-24.5	-15.0	-8.5	-3.8
3	BEN6	-480.0	-270.0	-105.0	-52.5	-27.0	-14.5	-6.1
4	DP50	-260.0	-155.0	-80.0	-45.0	-19.0	-8.4	-3.0
5	DP46i	-380.0	-210.0	-105.0	-53.0	-23.0	-12	-4.5
6	BereaUS1	-65.0	-45.0	-22.0	-17.5	-9.7	-6.0	-2.8
7	BereaUS5	-155.0	-100.0	-49.0	-34.0	-17.0	-9.2	-4.4
8	BEN7	-550.0	-285.0	-110.0	-55.5	-28.0	-15.0	-6.7

The SPC for all samples at different electrolyte concentrations is shown in Table 2. The electrical conductivity of the sample saturated by a fluid is obtained from the resistance measured by an impedance analyzer (Hioki IM3570) with the knowledge of the geometry of the sample (the length, the diameter) and is reported in Table 3. Based on the measured SPC with the knowledge of electrical conductivity of the samples (σ_r), formation factor, viscosity and dielectric constant, the zeta potential is deduced from equation 2 with an error margin of 15%. The main reasons of the error are that when pumping electrolytes through rocks, minerals of the rocks may dissolve. That leads to a slight change of electrical conductivity of fluid, permeability of rocks over time. Besides those, CO_2 intake from the air also influences the electrical conductivity, pH of the fluid. All above reasons contribute to the error

of the measured zeta potential. The zeta potential at different electrolyte concentrations is shown in Table 4. The result shows that for a given porous sample the zeta potential in magnitude increase with decreasing electrolyte concentration as displayed in Fig. 7. The observation is in good agreement with what is stated in literature [17, 34, 35].

Table 3. The electrical conductivity of the samples saturated by solutions (σ_r in mS/m) at different electrolyte concentrations.

	Sample ID	0.4 mM	1 mM	2.5 mM	5 mM	10 mM	20 mM	50 mM
1	BER5	1.9	2.6	3.5	5.4	7.9	13.6	26.1
2	BER502	1.6	2.2	3.4	6.0	8.4	14.5	28.3
3	BEN6	1.0	1.6	3.4	6.4	10.7	19.4	40.2
4	DP50	2.5	3.9	6.8	11.3	21.3	44.6	109.1
5	DP46i	2.1	2.9	5.4	10.1	17.1	31.2	68.4
6	BereaUS1	1.6	2.2	3.4	4.1	6.8	11.1	20.8
7	BereaUS5	1.4	2.0	3.5	4.6	8.8	15.1	30.6
8	BEN7	1.0	1.6	3.4	6.3	10.7	19.3	37.7

Table 4. The zeta potential of the samples (ζ in mV) deduced from equation 2 at different electrolyte concentrations.

	Sample ID	0.4 mM	1 mM	2.5 mM	5 mM	10 mM	20 mM	50 mM
1	BER5	-32.2	-29.4	-25.0	-23.4	-20.1	-19.5	-17.1
2	BER502	-38.6	-35.2	-30.0	-28.0	-24.1	-23.4	-20.5
3	BEN6	-82.2	-75.4	-61.0	-57.1	-49.0	-47.6	-41.4
4	DP50	-38.8	-36.1	-32.1	-30.1	-24.0	-22.2	-19.4
5	DP46i	-53.0	-40.4	-37.8	-35.5	-26.1	-24.8	-20.4
6	BereaUS1	-27.7	-26.1	-20.0	-19.1	-17.7	-17.8	-15.6
7	BereaUS5	-43.2	-39.9	-35.5	-32.1	-30.7	-28.4	-27.5
8	BEN7	-89.0	-81.6	-66.3	-61.8	-53.1	-51.5	-44.9

The values of the zeta potential deduced from our streaming potential measurements are consistent with those reported by [36] for St. Bees sandstone, by [37] for Stainton sandstone and Fountainbleau sandstone in the low-salinity domain (<0.25 M) as shown in Fig. 7. It is shown that the zeta potential against the electrolyte concentration has the trend with a regression as reported in [37] ($\zeta = a + b\log C_f$ with a = -9.67 mV, b = 19.02 mV and C_f is electrolyte concentration) and is displayed in Fig. 7 (solid line). It should be noted that there is another possibility for the zeta potential behavior deduced from a compilation of measurements performed on sandstones and sand [38, 39] in which the zeta potential is considered to be constant. The experimental result shows that the average value of the zeta potential for electrolyte concentrations above 0.01 M is about -23 mV. This value is comparable to a constant zeta potential of -17 mV from the work of [38, 39]. The experimental results also show that the zeta potential depends not only on the electrolyte concentration but also on types of rock. For example, the zeta potential for Bentheim Sandstones (BEN6 and BEN7) is nearly three times as high as that of Berea sandstone (BER5, BER502, BereaUS1 and BereaUS5) at the same electrolyte concentration.

The difference in the zeta potential can be explained by the difference in the surface site density, the disassociation constant for various types of porous rocks (see [34] for more details).

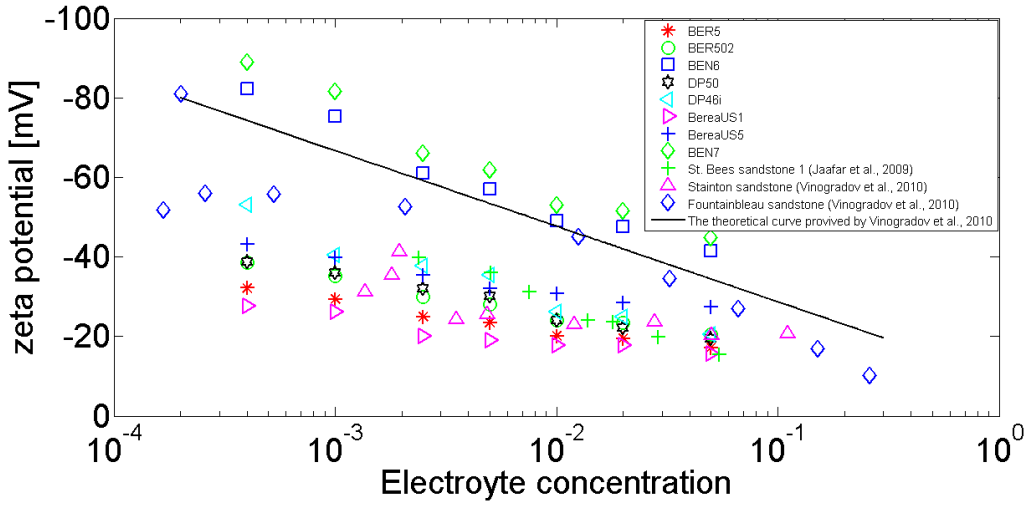

Figure 7. The zeta potential at different electrolyte concentrations (this work), Bees sandstone [36], Stainton sandstone and Fountainbleau sandstone [37]. The solid line is from an empirical expression obtained in [37] ($\zeta = a + b\log C_f$ with a = -9.67 mV, b = 19.02 mV).

5. Conclusions

The SPC measurements are carried out on 8 consolidated samples including both natural and artificial rocks saturated with 7 different NaCl solutions to determine the zeta potential. The experimental data of the zeta potential is then compared to previously published data for silica-based rocks. The comparison shows that the zeta potential deduced from the streaming potential measurements is in good agreement with the experimental data reported in the literature. The results indicate that the zeta potential depends not only on the electrolyte concentration but also on types of rock. For example, the zeta potential for Bentheim Sandstones (BEN6 and BEN7) is nearly three times as high as that of Berea sandstone (BER5, BER502, BereaUS1 and BereaUS5) at the same electrolyte concentration. The difference in the zeta potential can be explained by the difference in the surface site density, the disassociation constant for various types of porous rocks (mineral composition). This paper has also added to the existing experimental data of the zeta potential for various types of rock that is very important in electrokinetics.

Acknowledgments

This work has been carried out at the Van der Waals-Zeeman Institute/Institute of Physics, University of Amsterdam. We would like to thank Boris N. Kuvshinov (Shell) and Karel Heller (Delft University) for providing us the samples used in the experiments.

References

[1] L. Jouniaux, T. Ishido, International Journal of Geophysics (2012).
[2] B. Wurmstich, F. D. Morgan, Geophysics 59 (1994) 46–56.
[3] R. F. Corwin, D. B. Hoovert, Geophysics 44 (1979) 226–245.
[4] F. D. Morgan, E. R. Williams, T. R. Madden, Journal of Geophysical Research 94 (1989) 12.449–12.461.
[5] A. Revil, P. A. Pezard, Geophysical Research Letters 25 (1998) 3197– 3200.
[6] H. Mizutani, T. Ishido, T. Yokokura, S. Ohnishi, Geophys. Res. Lett. 3 (1976).
[7] M. Trique, P. Richon, F. Perrier, J. P. Avouac, J. C. Sabroux, Nature (1999) 137–141.
[8] A. A. Ogilvy, M. A. Ayed, V. A. Bogoslovsky, Geophysical Prospecting 17 (1969) 36–62.
[9] A. Thompson, S. Hornbostel, J. Burns, et al., SEG Technical Program Expanded Abstracts (2005).
[10] S. Haines, A. Guitton, B. Biondi, Geophysics 72 (2007) G1–G8.
[11] M. Strahser, L. Jouniaux, P. Sailhac, P. Matthey, M. Zillmer, Geophysical Journal International 187 (2011) 1378–1392.
[12] S. Garambois, M. Dietrich, Geophysics 66 (2001) 1417–1430.
[13] T. Paillat, E. Moreau, P.O.Grimaud, G. Touchard, IEEE Transactions on Dielectrics and Electrical Insulation 7 (2000) 693–704.
[14] C. Cameselle, K. R. Reddy, Electrochimica Acta 86 (2012) 10–22.
[15] C. Cameselle, S. Gouveia, D. E. Akretche, B. Belhadj, Organic Pollutants - Monitoring, Risk and Treatment, InTech, 2013.
[16] M. Ashraf, S. Tayyaba, N. Afzulpurkar, International Journal of Molecular Sciences 12 (2011) 3648–3704.
[17] B. J. Kirby, E. J. Hasselbrink, Electrophoresis 25 (2004) 187–202.
[18] O. Stern, Z. Elektrochem 30 (1924) 508–516.
[19] T. Ishido, H. Mizutani, Journal of Geophysical Research 86 (1981) 1763– 1775.
[20] H. M. Jacob, B. Subirm, Electrokinetic and Colloid Transport Phenomena, Wiley-Interscience, 2006.
[21] K. E. Butler, Seismoelectric effects of electrokinetic origin, PhD thesis, University of British Columbia, 1996.
[22] H. Hase, T. Ishido, S. Takakura, T. Hashimoto, K. Sato, Y. Tanaka, Geophysical Research Letters 30 (2003) 3197–3200.
[23] R. J. Hunter, Zeta Potential in Colloid Science, Academic, New York, 1981.
[24] B. Nourbehecht, Irreversible thermodynamic effects in inhomogeneous media and their applications in certain geoelectric problems, Ph.D. thesis, MIT Press, Cambridge, Mass, USA, 1963.
[25] A. Boleve, A. Crespy, A. Revil, F. Janod, J. L. Mattiuzzo, J. Geophys. Res. B08204 (2007).
[26] S. Dukhin, V. Shilov, Dielectric Phenomena and the Double Layer in Disperse Systems and Polyelectrolytes, John Wiley and Sons, New York, 1974.
[27] J. Davis, R. James, J. Leckie, Journal of Colloid and Interface Science 63 (1978).
[28] L. Jouniaux, M. L. Bernard, M. Zamora, J. P. Pozzi, Journal of Geophysical Research B 105 (2000) 8391–8401.
[29] P. Churcher, P. French, J. Shaw, L. Schramm, SPE International Symposium (1991).
[30] A. Pagoulatos, Evaluation of multistage Triaxial Testing on Berea sandstone, Degree of Master of Science, Oklahoma, 2004.
[31] A. A. Tchistiakov, Proceedings World Geothermal Congress (2000).
[32] D. Luong, R. Sprik, International Journal of Geophysics Article ID 471819 (2014).
[33] D. T. Luong, R. Sprik, Geophysical Prospecting (2015), accepted for publication.
[34] P. W. J. Glover, E. Walker, M. Jackson, Geophysics 77 (2012) D17–D43.
[35] P. Leroy, N. Devau, A. Revil, M. Bizi, Journal of Colloid and Interface Science 410 (2013).
[36] M. Z. Jaafar, J. Vinogradov, M. D. Jackson, Geophysical Research Letters 36 (2009) doi:10.1029/2009GL040549.
[37] J. Vinogradov, M. Z. Jaafar, M. D. Jackson, Journal of Geophysical Research 115 (2010) doi:10.1029/2010JB007593.
[38] V. Allegre, L. Jouniaux, F. Lehmann, P. Sailhac, Geophysical Journal International 182 (2010) 1248–1266.
[39] L. Jouniaux, Electrokinetic techniques for the determination of hydraulic conductivity in Hydraulic Conductivity - Issues, Determination and Applications, L. Elango, Ed., InTech, 2011